# Orbital Correlations in the Pseudocubic *O* and Rhombohedral *R* Phases of $\mathrm{LaMnO_3}$

Xiangyun Qiu,[1] Th. Proffen,[2] J. F. Mitchell,[3] and S. J. L. Billinge[1]

[1]*Department of Physics and Astronomy, Michigan State University, E. Lansing, Michigan 48824, USA*
[2]*Los Alamos National Laboratory, LANSCE-12, MS H805, Los Alamos, New Mexico 87545, USA*
[3]*Material Science Division, Argonne National Laboratory, Argonne, Illinois 60439, USA*

(Received 12 August 2004; revised manuscript received 24 February 2005; published 5 May 2005)

The local and intermediate structure of stoichiometric $\mathrm{LaMnO_3}$ has been studied in the pseudocubic and rhombohedral phases at high temperatures (300–1150 K). Neutron powder diffraction data were collected and a combined Rietveld and high real space resolution atomic pair distribution function analysis was carried out. The nature of the Jahn-Teller (JT) transition around 750 K is confirmed to be orbital order to disorder. In the high-temperature orthorhombic (*O*) and rhombohedral (*R*) phases, the $\mathrm{MnO_6}$ octahedra are still fully distorted locally. More importantly, the intermediate structure suggests the presence of local ordered clusters of diameter ~16 Å (~4 $\mathrm{MnO_6}$ octahedra) implying strong nearest-neighbor JT antiferrodistortive coupling. These clusters persist well above the JT transition temperature even into the high-temperature *R* phase.

DOI: 10.1103/PhysRevLett.94.177203 PACS numbers: 75.47.Lx, 61.12.−q, 75.47.Gk

The perovskite manganites related to $\mathrm{LaMnO_3}$ continue to yield puzzling and surprising results despite intensive study since the 1950s [1–3]. The pervading interest comes from the delicate balance between electronic, spin, and lattice degrees of freedom coupled with strong electron correlations. Remarkably, controversy still exists about the nature of the undoped endmember material, $\mathrm{LaMnO_3}$, where every manganese ion has a nominal charge of 3+ and no hole doping exists. The ground state is well understood as an A-type antiferromagnet with long-range ordered, Jahn-Teller (JT) distorted, $\mathrm{MnO_6}$ octahedra [4,5] that have four shorter and two longer bonds [6]. The elongated occupied $e_g$ orbitals lie down in the $xy$ plane and alternate between pointing along $x$ and $y$ directions, the so-called $O'$ structural phase [4,5]. At $T_{\mathrm{JT}} \sim 750$ K, the sample has a first-order structural phase transition to the *O* phase that formally retains the same symmetry but is pseudocubic with almost regular $\mathrm{MnO_6}$ octahedra (six almost equal bond lengths). In this phase the cooperative JT distortion has essentially disappeared. It is the precise nature of this *O* phase that is unclear. The *O* phase has special importance since it is the phase from which ferromagnetism and colossal magnetoresistance appear at low temperature at Ca, Sr dopings >0.2 [2,4].

Results on the *O* phase of $\mathrm{LaMnO_3}$ from different techniques are difficult to reconcile. On the one hand, greater electronic delocalization with an accompanying suppression of the *local* JT distortion explains well transport [7,8], magnetic [8,9], and crystallographic [10] observations, whereas probes of local structure [11–13] favor robust JT distortions persisting in the *O* phase implying charge localization. A full understanding of this important parent phase is clearly lacking. Here we use a diffraction probe of the local and intermediate range atomic structure, neutron pair distribution function (PDF) analysis, to reconcile the local and average behavior. This method allows quantitative structural refinements to be carried out on intermediate length scales in the nanometer range. We confirm that the JT distortions persist, unchanged, locally at all temperatures, and quantify the amplitude of these *local* JT distortions. No local structural study exists of the high-temperature rhombohedral *R* phase that exists above $T_R = 1010$ K. We show for the first time that, even in this phase where the octahedra are constrained by symmetry to be undistorted, the local JT splitting persists. More significantly, fits of the PDF over different $r$ ranges indicate that locally ordered domains of distorted octahedra of diameter ~16 Å persist in the *O* phase. This is the first observation of such locally correlated, short-range ordered octahedra in the manganites. The clusters are robust and persist to the highest temperatures (1150 K), only growing in size as $T_{\mathrm{JT}}$ is approached on cooling. Finally, we show that the crystallographically observed volume reduction at $T_{\mathrm{JT}}$ [10] is not due to the reduction in average Mn-O bond length observed crystallographically. However, it is consistent with increased octahedral rotational degrees of freedom.

Powder samples of ~6 g were prepared from high purity $\mathrm{MnO_2}$ and $\mathrm{La_2O_3}$; the latter was prefired at 1000 °C to remove moisture and carbon dioxide. Final firing conditions were chosen to optimize the oxygen stoichiometry at 3.00. The crystallographic behavior was confirmed by Rietveld refinements using program GSAS [14]. Both the differential thermal analysis and Rietveld measurements estimated the same phase transition temperatures of $T_{\mathrm{JT}} \sim 735$ K and $T_R \sim 1010$ K. These values indicate that the sample is highly stoichiometric [5,15]. Neutron powder diffraction data were collected on the NPDF diffractometer at the Lujan Center at Los Alamos National Laboratory. The sample, sealed in a cylindrical vanadium tube under an helium gas atmosphere, was measured from 300 to 1150 K. A final measurement at 300 K confirmed that the sample was unchanged by the thermal cycling in reducing atmosphere. Data reduction to obtain the PDFs [16] was carried out using the program PDFGETN [17]. PDF modeling was carried out using the program PDFFIT [18].

We first confirm the earlier extended x-ray absorption fine structure results [11,12] and establish that in the $O$ phase the full JT distortion persists in the local structure. This result can be seen qualitatively in Fig. 1. In panel (a) the first peak in the PDF, coming from Mn-O nearest-neighbor bonds, is shown. This peak is upside down because of the negative neutron scattering length of Mn [16]. It is double valued because of the presence of shorter bonds of average length 1.94 Å, and long bonds of length 2.16 Å [indicated by dashed lines in Fig. 1(a)], coming from the JT distorted octahedra. The doublet is clearly evident at low temperature below $T_{\mathrm{JT}}$. However, the splitting persists up to the highest temperature and remains larger than the thermal broadening of the peaks. This shows qualitatively and intuitively that the JT distortion survives at all temperatures. The peaks do broaden at the higher temperature due to increased thermal motion [16] and the two contributions to the doublet are not resolved at the high temperature. However, it is clear that the peak is not the broad, single valued, Gaussian at high temperatures predicted by the crystallographic models.

We would like to see if there is any change in the peak profile on crossing the $T_{\mathrm{JT}}$ beyond normal thermal broadening. To test this, we plot the change in this nearest-neighbor Mn-O peak between $T = 720$ K and $T = 880$ K, as it crosses $T_{\mathrm{JT}}$, and compare this to the change in the peak on going from 650 to 720 K. The latter case has approximately the same temperature differential (thermal broadening will be comparable) but there is no structural transition in that range. The difference curves from these two situations, shown in Fig. 1(b), are almost identical. We conclude that there is virtually no change to the $MnO_6$ octahedra as they go from the $O'$ to the $O$ phase and that the bulk of the sample remains JT distorted.

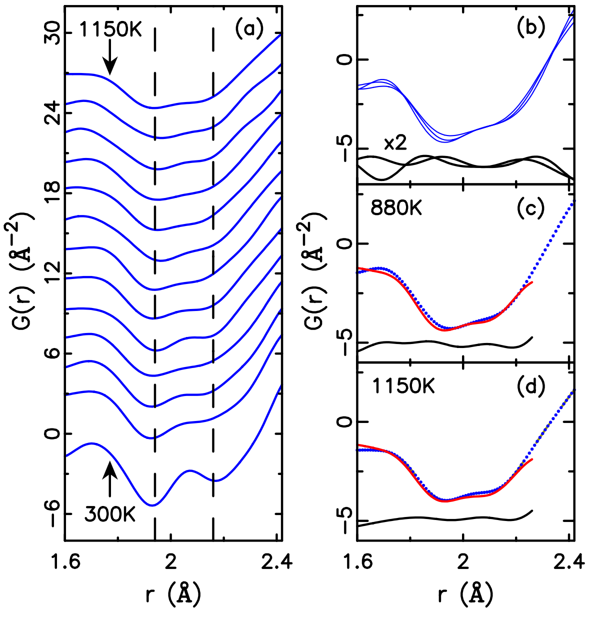

FIG. 1 (color online). (a) Low-$r$ region of the experimental PDFs at all temperatures offset along the $y$ axis with increasing temperature. Two dashed lines indicate the Mn-O short and long bonds at 1.94 and 2.16 Å, respectively. (b) PDFs at 650, 720, and 880 K without offset. The differences between 720 and both 650 and 880 K (both high $T$ minus low $T$) are shown offset below. (c) Two-Gaussian fit of PDF data at 880 K (solid dots). The solid line denotes fitted curve with the difference curve offset below. (d) Same as (c) for 1150 K PDF data.

Finally, to quantify the nature of the local JT distortions, we have fit two Gaussian peaks to the nearest-neighbor $MnO_6$ doublet in the experimental data at all temperatures. The quality of the fits at "low" (880 K) and high (1150 K) temperature are rather good, as can be seen in Figs. 1(c) and 1(d). The position and width of each peak, and the total integrated intensity of the doublet, were allowed to vary (the intensities of the long and short bond distributions were constrained to be 1:2 in the fits). The weighted residual factor $R_{wp}$ varies from 1% at high temperature to 5% at low temperature indicating excellent agreement over all temperatures. Attempts to fit a single Gaussian in the $O$ phase resulted in significantly worse agreements. The results of the temperature-dependent fits are shown in Fig. 2. No anomaly of any kind can be identified across the $T_{\mathrm{JT}} = 735$ K. The integrated intensities and peak positions do not change significantly with temperature from 300 to 1150 K indicating that the average bond lengths of the short and long bonds are rather temperature independent. This also implies that essentially all the octahedra remain JT distorted [19]. The peak widths increase slightly with temperature due to increased thermal motion [Fig. 2(b)]; however, there is no clear discontinuity in the peak broadening associated with the phase transition. The results confirm that the *local* JT distortions persist, virtually unstrained, into the $O$ and $R$ phases.

Models were refined to the data over different ranges of $r$. Fits confined to the low-$r$ region will yield the local (JT

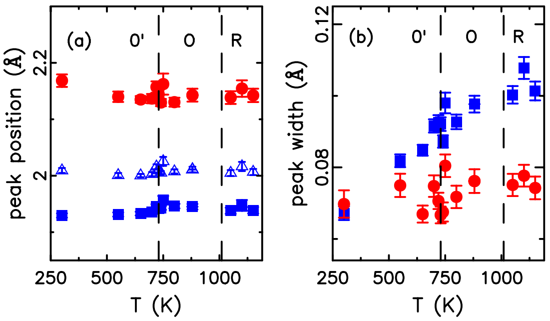

FIG. 2 (color online). Fitting results of the Mn-O PDF peaks with two Gaussians: the low-$r$ peak (■) around 1.94 Å; the high-$r$ peak (●) ~2.16 Å. The open triangles are the weighted average, $\langle r_{\mathrm{Mn\text{-}O}} \rangle$. The dashed lines denote the phase transition temperatures. (a) Peak positions; (b) peak widths.

distorted) structure whereas fits over wider ranges of $r$ will gradually cross over to the average crystallographic structure. To extract the size of the short-range ordered clusters, we have fit the PDF from $r_{\mathrm{min}} = 1.5$ Å to $r_{\mathrm{max}}$, where $r_{\mathrm{max}}$ was increased step by step from 5 to 20 Å, by which time the PDF refinement agrees with the average structure refinement from Rietveld. This was done for all data sets. The model used at all temperatures was the low-temperature structure in the *Pbnm* space group. Representative results are shown as open circles in Fig. 3. Note that three distinct bond lengths are obtained from modeling although only two peaks can be resolved directly in the PDF at low $r$. The amplitude of the refined JT distortion is constant as a function of $r_{\mathrm{max}}$ at 300 K reflecting the fact the orbital order is perfectly long range [Fig. 3(a)]. At higher temperature, and especially in the $O$ phase, the amplitude of the refined distortion falls off smoothly as the fit range is extended to higher $r$, until it asymptotically approaches the much smaller crystallographically refined value. We understand this behavior in the following way. Domains of local orbital order exist in the $O$ phase. These may resemble the pattern of orbital order at low temperature ($O'$ phase), and for convenience this is how we have modeled them. These domains do not propagate over long range and are orientationally disordered in such a way that, on average, the observed pseudocubic structure is recovered. We can estimate the domain size by assuming that the orbitals are ordered inside the domain but uncorrelated from one domain to the neighboring domain. This results in a falloff in the amplitude of the refined distortion with increasing fit range with a well defined PDF form factor [20], assuming spherical domains, that depends only on the diameter of the domain. The three curves of refined bond length vs $r_{\mathrm{max}}$ from the short, medium, and long bonds of the $\mathrm{MnO_6}$ octahedron could be fit at each temperature with the diameter of the domain as the *one single* parameter. Representative fits are shown in Fig. 3 as the solid lines. The temperature dependence of the inverse domain diameter is shown in Fig. 4(a). We find that in the pseudocubic $O$ phase these clusters have a diameter of ~16 Å, roughly independent of temperature except close to $T_{\mathrm{JT}}$ where the size grows. Below $T_{\mathrm{JT}}$ the correlation length of the order is much greater, although some precursor effects are evident just below $T_{\mathrm{JT}}$. The refined domain size of orbital order is similar in the $R$ phase though the quality of the fits becomes worse in this region. This may be because the nature of the short-range orbital correlations changes, i.e., becomes different from the $O'$ phase. The correlation length scale of 16 Å spans over four $\mathrm{MnO_6}$ octahedra, suggesting strong nearest-neighbor JT antiferrodistortive coupling (as expected from the fact that neighboring $\mathrm{MnO_6}$ octahedra share one oxygen atom) and weak second and higher nearest-neighbor coupling.

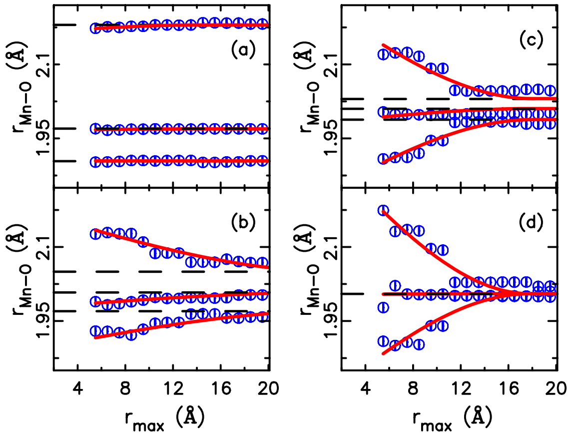

FIG. 3 (color online). Mn-O bond lengths from the refined structure model as a function of $r_{\mathrm{max}}$ are shown as circles. Error bars are smaller than, but comparable to, the symbol size. The solid lines (colored red online) are the expected behavior assuming spherical locally ordered clusters. All three bond lengths are self-consistently fit with a single parameter, the cluster size. The horizontal dashed lines indicate the Mn-O bond lengths from Rietveld refinements. (a) 300 K; (b) 740 K; (c) 800 K; (d) 1100 K.

The orientational disorder of the JT distorted $\mathrm{MnO_6}$ octahedra gives the $O$ phase its pseudocubic nature over the long range. Crystallographic average structure modeling, which results in nearly regular $\mathrm{MnO_6}$ octahedra, accounts for this disorder through increased thermal displacement parameters (TDP). The same behavior is seen in wide $r$-range PDF modeling fits which are in good agreement with the crystallography. The largest response should be seen in the oxygen TDP in a direction parallel to the Mn-O bond reflecting the larger static bond length distribution in this direction (there are a mixture of long and short bonds in each direction in the disordered phase). This is clearly seen in the anisotropic TDPs refined from wide-$r$

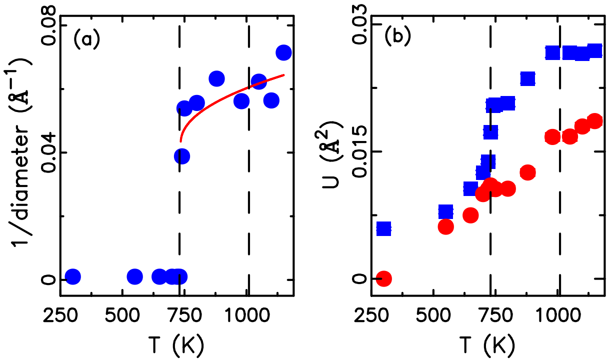

FIG. 4 (color online). (a) Inverse of the domain diameter obtained from the fits shown in Fig. 3. The solid line is a simple exponential curve fit as a guide to the eye. (b) Thermal displacement parameters of oxygen atoms parallel (blue ■) and perpendicular (red ●) to Mn-O bonding directions. The perpendicular component (●) is shifted down by 0.007 Å$^2$ for clarity.

range PDF fits shown in Fig. 4(b) (blue ■). The TDP increases discontinuously at the $O'$-$O$ phase line reflecting where the JT distorted octahedra first become orientationally disordered.

We might also expect a response in the TDPs perpendicular to the Mn-O bonds reflecting increased inhomogeneous octahedral tilting that will appear to accommodate the strain as the JT distorted octahedra become orientationally disordered. There is no discontinuous change in this parameter at $T_{JT}$ [Fig. 4(b), red ●]. Our current PDF results explain this to some extent. The JT distorted octahedra remain locally orientationally short-range ordered with the orbital correlations dying out over a range of ~2 nm. We speculate that in this way the structure gains most of the entropy gain of disordering the octahedra while minimizing inhomogeneous strain.

We now address the issue of the unit-cell volume collapse observed crystallographically [10] at $T_{JT}$. Our Rietveld refinements show this to be due to a shortening of the average Mn-O bond length $\langle r_{\text{Mn-O}} \rangle$ by 0.0093(1) Å. This results in a reduction in the average volume of the $MnO_6$ octahedra which has been used as evidence to support an increase in charge delocalization with increasing temperature at this transition [10]. Our wide $r$-range PDF fits agree with this result, yielding a shortening of $\langle r_{\text{Mn-O}} \rangle$ of 0.0082(13) Å. However, the low-$r$ PDF fits do not support this reduction in volume of the $MnO_6$ octahedra at $T_{JT}$. Locally, $\langle r_{\text{Mn-O}} \rangle$ *increases* smoothly with temperature. This is evident in Fig. 2(a) (open triangles). A fit to these points yields a thermal expansion coefficient for the Mn-O bond of $+1.7(9) \times 10^{-5}$ Å/K. There is clearly no discontinuous shortening of this bond of order 0.01 Å at $T_{JT}$. The local bond lengthening, yet average shortening, can be reconciled if there is an increase in the average octahedral tilt angle at $T_{JT}$. We do not see this directly in our refinements but the magnitude is expected to be very small (the average tilt angle needs to increase by 0.4 degrees to account for the observed 0.38% volume collapse) and below our experimental sensitivity. In summary, the PDF data clearly show that the volume collapse at $T_{JT}$ is not due to a shortening of $\langle r_{\text{Mn-O}} \rangle$. We postulate that a small increase in the average octahedral tilt angle would explain this result but do not have direct evidence for this.

The sudden increase of conductivity across the JT transition [7,8] cannot be easily explained by the locally JT distorted $MnO_6$ octahedra and increased octahedral tilt in the high-temperature phase. We speculate that this conductivity anomaly comes along with the dynamic nature of the JT distortions. Zhou and Goodenough have proposed a vibronic model where some $Mn^{3+}$ ions charge disproportionate into $Mn^{2+}$ and $Mn^{4+}$ [8]. The increased conductivity would enhance the ferromagnetic correlations [8,9]. We see no direct evidence for this charge disproportionation but if it occurs on a small minority of sites it would be undetectable in our data.

In summary, the PDF clearly shows that the JT transition in $LaMnO_3$ is of orbital order-disorder type. More importantly, we found that 16 Å nanoclusters of short-range orbital order persist in the high-temperature $O$ and $R$ phases. Our analysis of the PDF shows that this is a promising approach to extract nanocluster information in the absence of single crystal diffuse scattering data and in cases such as this where no scattering contrast exists for small angle scattering to probe the nanoclusters.

Work at MSU was supported by NSF through Grant No. DMR-0304391. Work at ANL was supported by DOE under Contract No. W-31-109-ENG-38. Beamtime on NPDF at Lujan Center was funded by DOE through Contract No. W-7405-ENG-36.

[1] A. J. Millis, Phys. Rev. B **53**, 8434 (1996); M. B. Salamon and M. Jaime, Rev. Mod. Phys. **73**, 583 (2001).
[2] A. P. Ramirez, J. Phys. Condens. Matter **9**, 8171 (1997).
[3] G. C. Milward, M. J. Calderón, and P. B. Littlewood, Nature (London) **433**, 607 (2005); E. Dagotto *et al.*, *Nanoscale Phase Separation and Colossal Magnetoresistance* (Springer-Verlag, Amsterdam, 2003).
[4] E. O. Wollan *et al.*, Phys. Rev. **100**, 545 (1955).
[5] J. Rodríguez-Carvajal *et al.*, Phys. Rev. B **57**, R3189 (1998).
[6] Th. Proffen, R. G. DiFrancesco, S. J. L. Billinge, E. L. Brosha, and G. H. Kwei, Phys. Rev. B **60**, 9973 (1999).
[7] P. Mandal, B. Bandyopadhyay, and B. Ghosh, Phys. Rev. B **64**, 180405 (2001).
[8] J.-S. Zhou and J. B. Goodenough, Phys. Rev. B **60**, R15002 (1999).
[9] M. Tovar *et al.*, Phys. Rev. B **60**, 10199 (1999).
[10] T. Chatterji, F. Fauth, B. Ouladdiaf, P. Mandal, and B. Ghosh, Phys. Rev. B **68**, 052406 (2003).
[11] E. Araya-Rodriguez *et al.*, J. Magn. Magn. Mater. **233**, 88 (2001).
[12] M. C. Sánchez, G. Subías, J. García, and J. Blasco, Phys. Rev. Lett. **90**, 045503 (2003).
[13] E. Granado, J. A. Sanjurjo, C. Rettori, J. J. Neumeier, and S. B. Oseroff, Phys. Rev. B **62**, 11304 (2000).
[14] A. C. Larson and R. B. Von Dreele, GSAS Report No. LAUR-86-748, Los Alamos National Laboratory.
[15] P. Norby *et al.*, J. Solid State Chem. **119**, 191 (1995).
[16] T. Egami and S. J. L. Billinge, *Underneath the Bragg Peaks: Structural Analysis of Complex Materials* (Pergamon, Elsevier, 2003).
[17] P. F. Peterson *et al.*, J. Appl. Crystallogr. **33**, 1192 (2000).
[18] Th. Proffen and S. J. L. Billinge, J. Appl. Crystallogr. **32**, 572 (1999).
[19] Undistorted octahedra at the level of ~1% would not be visible in our data.
[20] M. Lei, Ph.D. thesis, Michigan State University, 2003.